Alma Mater Studiorum Università di Bologna
Archivio istituzionale della ricerca

RSS-Based Localization of Multiple Radio Transmitters via Blind Source Separation

(Article begins on next page)

10 November 2024

RSS-based Localization of Multiple Radio Transmitters via Blind Source Separation

Enrico Testi, *Student Member, IEEE,* Andrea Giorgetti, *Senior Member, IEEE*

Abstract—This letter proposes a methodology for counting and locating the nodes of an uncooperative wireless network using power measurements collected by sensors. The approach is blind, allowing the detection and localization of the nodes without knowing the network's specific features (i.e., the number of nodes, modulation type, and medium access control (MAC)). Because the signals captured by the radio-frequency (RF) sensors are additively mixed, blind source separation (BSS) is used to separate transmitted power profiles. Then, received signal strength (RSS) is extracted from the reconstructed signals and localization is performed through conventional least square (LS) and maximum likelihood (ML) techniques. Numerical results reveal that the BSS-ML approach reaches a rather low localization error in mild shadowing regimes, even when the ratio between the number of RF sensors and nodes, ρ, is close to 1. Finally, it is shown how the performance degradation introduced by the imperfect BSS is slight and that the root mean square error (RMSE) approaches the Cramér–Rao lower bound (CRLB) when increasing ρ.

Index Terms—Blind source separation, principal component analysis, received signal strength, localization, maximum likelihood estimation, least squares estimation.

I. INTRODUCTION

LOCATION-AWARE technologies are deemed to enhance wireless network capabilities and pave the way to new unforeseen applications. Let us consider a scenario in which a wireless network periodically senses the radio-frequency (RF) spectrum collecting simple over-the-air power samples and detecting and localizing all the transmitters in the area. Such information can then be used to make intelligent decisions for dynamic spectrum access [1]. Furthermore, in the context of defense operations, understanding the structure of the enemy's network may increase spectrum awareness. In this sense, a network of RF sensors can be spread within an unknown environment to detect and collect helpful information about the adversarial network structure [2], [3], [4]. An unusual condition of such applications is that they imply that the detection and localization of unknown network nodes are performed without having the chance to be part of it.

There have been several fundamental contributions on localization over the past decade exploiting different technologies, such as WiFi and ultrawide band (UWB) [5], [6], [7], [8]. Furthermore, the problem of multi-target localization using groups of cooperating sensors has also been widely investigated [9], [10], including an original framework that ensure scalability

and distributed implementation [6]. However, all the above works assume that the targets can exchange information with the anchors, thus contributing to the localization process. In [11], the authors propose a particle simulation algorithm for the localization of wireless transmitters leveraging on a large number of RF sensors distributed on a grid.

This letter proposes a novel methodology for counting and locating the nodes of a packet-based non-collaborative wireless network using over-the-air power profiles captured by RF sensors. In particular, the sensors do not have access to the target network and ignore its main features (i.e., the number of nodes, modulation type, and medium access control (MAC)). Hence, the RF sensors can only measure the aggregate power received by the nodes. Then, a fusion center processes the power measurements to estimate the number and position of the nodes. This problem is challenging because nodes may transmit simultaneously in the same frequency band, sensors can be placed in an unfavorable geometrical configuration, and sensing is hindered by path-loss, shadowing, and measurement noise. Regarding the first challenging aspect, the RF sensors receive a mixture of signals, so blind source separation (BSS) is used to separate traffic patterns.

The processing chain depicted in Fig. 1 shows the stages of the algorithm, while an example of a typical scenario is shown in Fig. 3. Firstly, a BSS is performed to count the number of targets and reconstruct the power profiles transmitted by each of them. Then, through a non-linear filtering procedure, the received signal strength (RSS) associated with each sensor-target couple is extracted. After this filtering step, the sensors can localize the target nodes separately using any conventional positioning technique based on RSS. For instance, in this work, localization is performed through least square (LS) and maximum likelihood (ML) techniques. In the numerical results, the performance of the methodology is derived in different shadowing regimes and varying the sensors' spatial density, and it is compared with the solution proposed in [11].

The remainder of this letter is organized as follows. Section II describes the scenario, the system model, and the proposed framework. In Section III the adopted localization algorithms are briefly introduced. Numerical results are shown in Section IV. Throughout the paper, lowercase bold letters denote vectors, capital boldface letters denote matrices, the transpose operator is represented by $(\cdot)^{\mathsf{T}}$, and $||\cdot||_p$ is the l_p-norm. With $v_{i,j}$ and $\mathbf{v}_i$ we represent, respectively, the element and the ith row of the matrix $\mathbf{V}$. The shorthand $\mathcal{N}(\mu, \sigma^2)$ is used to denote a real Gaussian distribution with mean μ and variance σ^2, while $\mathbb{1}_{\{\mathcal{A}\}}$ is the indicator function equal to one when $\mathcal{A}$ is true and zero otherwise.
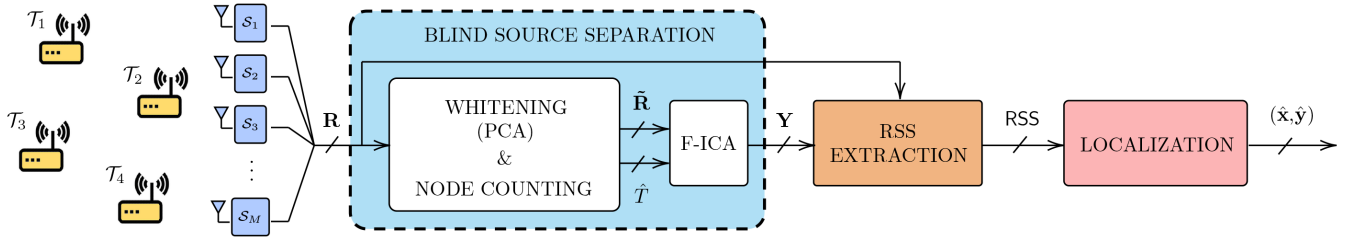
Fig. 1. Block scheme of the complete methodology: target nodes ($\mathcal{T}_1, \mathcal{T}_2, \ldots$), RF sensors ($\mathcal{S}_1, \mathcal{S}_2, \ldots$), node counting (principal component analysis (PCA)), received power profiles separation (fast independent component analysis (F-ICA)), transmitted power profile reconstruction (RSS extraction), and localization.

II. Blind Source Separation

Let us consider a set $\mathcal{T}$ of target nodes of a wireless network at unknown positions and a set $\mathcal{S}$ of RF sensors at known locations. Let T and S be the cardinality of $\mathcal{T}$ and $\mathcal{S}$, respectively.

Due to the packet-based communication, the transmission power of a node calculated over short time intervals (called bins) of duration T_b is a random on/off process representing the transmission power profile of that node. Let us arrange such profiles as rows of a matrix $\mathbf{P} \in \mathbb{R}^{T \times K}$ whose element $p_{t,k}$ indicate the transmit power of node t at time bin k with $t = 1, 2, \ldots, T$ and $k = 1, 2, \ldots, K$, where K is the number of samples collected over a period of time $T_{\mathrm{ob}} = K T_b$ (namely the observation time).

The sensors $\mathcal{S}$ gather the power received from the nodes and sample it through an energy detector (ED), consisting of a bandpass filter with bandwidth W, followed by a square-law device and an integrator with finite integration time T_b [12], [13]. The result of this operation is a matrix $\mathbf{R} \in \mathbb{R}^{S \times K}$ of received powers, $r_{s,k}$, related with $\mathbf{P}$ by[1]

$$\mathbf{R} = \mathbf{HP} + \mathbf{N} \tag{1}$$

where $\mathbf{H} \in \mathbb{R}^{S \times T}$ is the matrix of channel power gains, $h_{s,t}$, and $\mathbf{N} \in \mathbb{R}^{S \times K}$ is the matrix of noise power samples, $n_{s,k}$, at the sensors, due to thermal noise. The channel gain between target node t and sensor s consists of two terms $h_{s,t} = h'_{s,t} e^{\sigma g_{s,t}}$, where $h'_{s,t}$ accounts for path-loss and $g_{s,t} \sim \mathcal{N}(0,1)$ is a random variable (r.v.) to model log-normal shadowing with intensity σ [14].[2] The path-loss model is of power-law type with channel gain $h'_{s,t} = h_0 (\frac{d_0}{d_{s,t}})^\nu$ where ν is the path-loss exponent, h_0 is the channel gain at the reference distance d_0, and $d_{s,t}$ is the distance between sensor s and node t. The power noise samples $n_{s,k}$ are independent, identically distributed (i.i.d.) central chi-squared r.v.s with a number of degrees of freedom $N_{\mathrm{dof}} = 2W T_b$. When $N_{\mathrm{dof}} \gg 1$ by the central limit theorem $n_{s,k} \sim \mathcal{N}(\sigma_{\mathrm{n}}^2, 2\sigma_{\mathrm{n}}^4/N_{\mathrm{dof}})$, where $\sigma_{\mathrm{n}}^2 = 2N_0 W$ [12].

To localize the nodes $\mathcal{T}$ using a RSS-based method, it is thus necessary to recover the transmitted power profiles $\mathbf{P}$ from the mixture $\mathbf{R}$ observed by sensors $\mathcal{S}$ (see (1)). Since we can only observe over-the-air power received by the RF sensors, we propose BSS to extract the sources from the mixtures.

A. Whitening and Source Counting

Before separating the sources, it is necessary to know their number, T, and pre-process the data $\mathbf{R}$ to reduce its dimensionality (from S to T) and get T mixtures centered and whitened. Since the features of the target network are unknown, it is required to estimate the number of nodes, T. Both the estimation of the number of nodes and dimensionality reduction can be performed by principal component analysis (PCA).

The first pre-processing operation is centering, which refers to subtracting the mean from the data. In practice, the row-wise mean is removed from the matrix of the mixed signals $\mathbf{R}$. Then, by performing eigenvalue decomposition of the sample covariance matrix $\mathbf{\Sigma} = \frac{1}{K} \mathbf{RR}^\mathsf{T} = \mathbf{U \Lambda U}^\mathsf{T}$, the matrix of the eigenvectors $\mathbf{U}$, and the diagonal matrix of the eigenvalues $\mathbf{\Lambda}$ are obtained. The eigenvalues Λ_i, with $i = 1, 2, \ldots, S$, are thus sorted in descending order along with the corresponding eigenvectors. The number of sources generating the mixture is given by the number of significant eigenvalues, i.e.,

$$\widehat{T} = \sum_{i=1}^{S} \mathbb{1}_{\{\Lambda_i > \bar{\Lambda}\}} \tag{2}$$

with $\bar{\Lambda} = w \cdot (\Lambda_1 - \Lambda_S)$, where $w \in [0,1]$ is the eigenvalue selection parameter chosen, e.g., according to the scree plot approach [15].

To decorrelate the data in preparation of the subsequent separation, a linear transformation named whitening, is prformed by the whitening matrix $\mathbf{Q}$

$$\mathbf{Q} = \mathbf{\Lambda}^{-\frac{1}{2}} \mathbf{U}^\mathsf{T}. \tag{3}$$

Retaining only the $\widehat{T}$ largest eigenvalues and the corresponding eigenvectors in (3), a reduced projection matrix, $\tilde{\mathbf{Q}}$, is obtained. Therefore, the mixed signals can be projected onto a subspace whose dimensionality is reduced from S to $\widehat{T}$ by

$$\tilde{\mathbf{R}} = \tilde{\mathbf{Q}} \mathbf{R}. \tag{4}$$

B. Independent Component Analysis

Independent component analysis (ICA) is a method to find a linear representation of non-Gaussian data so that the components are statistically independent. Here we apply ICA to unmix the transmitted power profiles (implicitly contained in $\mathbf{P}$). In particular, ICA allows us to estimate the unmixing matrix $\mathbf{W} \in \mathbb{R}^{\widehat{T} \times \widehat{T}}$ such that

$$\mathbf{Y} = \mathbf{W}^\mathsf{T} \tilde{\mathbf{R}} \tag{5}$$

---

[1]Assuming the received signals and noise are uncorrelated.
[2]Without loss of generality the r.v.s $g_{s,t}$ are considered independent.
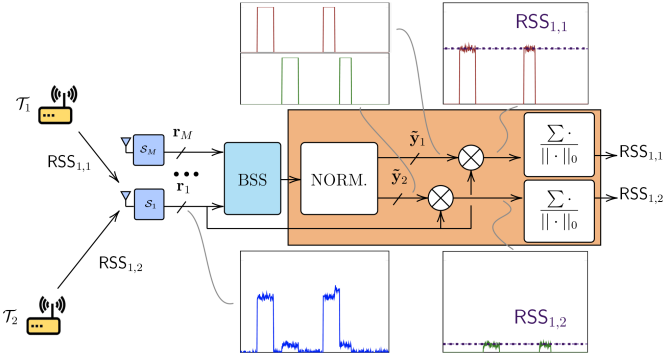
Fig. 2. The RSS extraction process for two non-collaborative transmitters.

where $\mathbf{Y} \in \mathbb{R}^{\widehat{T} \times K}$ is the matrix of the separated temporal power profiles. If BSS were ideal, the matrix $\mathbf{Y}$ would coincide with the transmitted power profiles $\mathbf{P}$ as if we were able to tap the signals directly from the transmitting antennas. In this work, we propose using F-ICA, an iterative algorithm based on two constituents: kurtosis to measure non-Gaussianity, and Gram-Schmidt orthogonalization to perform decorrelation [16].

C. RSS Extraction

Although the F-ICA technique applied in the power-domain suits this scenario, it presents a relevant issue. The reconstructed signals are scaled and do not preserve the original power. For this reason, another processing stage is necessary to perform the RSS-based localization.

Let us normalize the reconstructed power profiles $\mathbf{Y}$ such that $\tilde{\mathbf{Y}}$ has elements $\tilde{y}_{t,k} = 1$ if node t is transmitting in the k-th bin, and $\tilde{y}_{t,k} = 0$ otherwise. Such normalization can be performed via thresholding, i.e.,

$$\tilde{y}_{t,k} = \mathbb{1}_{\{y_{t,k} \geq \lambda_t\}} \tag{6}$$

where $\lambda_t = q \cdot \max_k\{y_{t,k}\}$ is a normalization threshold chosen as a fraction $q \in [0,1]$ of the maximum power of the transmit profile of target node t. Thus, each row $\tilde{\mathbf{y}}_t$ can be seen as a mask that, multiplied element-wise by the s-th row of $\mathbf{R}$, $\mathbf{r}_s$, forces to zero all the power samples received by sensor s that have not been transmitted by node t. Fig. 2 depicts the procedure with an example of two partially overlapped transmissions, where the normalized reconstructed power profile $\tilde{\mathbf{y}}_1$, when multiplied element-wise by, e.g., $\mathbf{r}_1$, forces to zero all the power samples received by sensor $\mathcal{S}_1$ that have not been transmitted by node $\mathcal{T}_1$. Then, the received signal strength between the target node t and the sensor s, $\mathsf{RSS}_{s,t}$, is obtained by averaging over the non-zero entries of the result of the element-wise product. Such process can be expressed in a compact form as

$$\mathsf{RSS}_{s,t} = \frac{\sum_{k=1}^{K} r_{s,k}\, \tilde{y}_{t,k}}{\|\mathbf{r}_s \odot \tilde{\mathbf{y}}_t\|_0} \qquad s = 1, \ldots, S \ \ t = 1, \ldots, T, \tag{7}$$

where $\odot$ stands for the element-wise product. The averaging ensures that the RSS is estimated within a time frame of duration T_{ob}.

III. LOCALIZATION

The position estimation is obtained through a two-dimensional RSS-based localization algorithm.[3] Let us assume the targets are located at unknown coordinates (x_t, y_t) with $t = 1, \ldots, T$ and the RF sensors are at known positions $(\tilde{x}_s, \tilde{y}_s)$ with $s = 1, \ldots, S$. In this work, two well-known solutions for the localization of single targets (the generic node t in the following) are considered.

Least Squares Localization. Let us build a matrix $\mathbf{B}$, that contains RSS measurements obtained through (6)-(7) and the sensors position, with rows $\mathbf{b}_s = (2\tilde{x}_s, 2\tilde{y}_s, \mathsf{RSS}_{s,t}^{-1/\nu}, -1)$ for $s = 1, \ldots, S$, and a vector $\mathbf{q} = (\tilde{x}_1^2 + \tilde{y}_1^2, \ldots, \tilde{x}_S^2 + \tilde{y}_S^2)^{\mathsf{T}}$. Let us also define the two unknowns, $D^2 = x_t^2 + y_t^2$ and $P = (P_{\mathrm{tx}} h_0)^{\frac{1}{\nu}}$, where P_{tx} is the transmit power of the nodes. By ordinary LS method the solution is [17]

$$\hat{\mathbf{p}} = \arg\min_{\mathbf{p} \in \mathbb{R}^4}\{\|\mathbf{B}\mathbf{p} - \mathbf{q}\|_2^2\} = (\mathbf{B}^{\mathsf{T}}\mathbf{B})^{-1}\mathbf{B}^{\mathsf{T}}\mathbf{q} \tag{8}$$

where $\mathbf{p} = (x_t, y_t, P, D^2)^{\mathsf{T}}$.

Maximum Likelihood Localization. Without any prior statistical knowledge about the transmit power and location, the ML estimation of the t-th target location is given by [18], [17]

$$(\hat{x}_t, \hat{y}_t) = \arg\min_{(x_t, y_t) \in \mathbb{R}^2}$$
$$\left\{ \sum_{i=1}^{S} \left(\ln\left(\mathsf{RSS}_{i,t} d_{i,t}^{2\nu}\right) - \frac{1}{S} \sum_{j=1}^{S} \ln\left(\mathsf{RSS}_{j,t} d_{j,t}^{2\nu}\right) \right)^2 \right\} \tag{9}$$

where $d_{i,t} = \sqrt{(x_t - \tilde{x}_i)^2 + (y_t - \tilde{y}_i)^2}$. The objective function (9) is differentiable with respect to (x_t, y_t), hence it is possible to find the minimum in closed form or via the gradient descent method. However, if the target nodes are arranged in an unfavorable configuration, there can be several local minima. For this reason, the monitored area has been discretized into a two-dimensional grid, and the grid point that gives the minimum value of (9) is chosen. The finer the grid, the more accurate the estimation is at the cost of an increased computational burden.

IV. NUMERICAL RESULTS

In this section, the performance of the proposed methodology is evaluated in realistic scenarios accounting for the random deployment of nodes and sensors, sensor spatial density, and channel impairments. All the results are obtained through an ad-hoc network simulator developed for the *ns3* platform.

A. Parameter Setting and Simulation Setup

Both the target and the sensor nodes are deployed within a square area of side $L = 50\,\mathrm{m}$. The target nodes belong to an ad-hoc network operating at $f_0 = 2.412\,\mathrm{GHz}$ compliant with the IEEE $802.11s$ standard and all of them use the same frequency channel. The RF sensors have bandwidth of $W = 20\,\mathrm{MHz}$ and continuously sense the spectrum, with an ED integration time of $T_{\mathrm{b}} = 10\,\mu\mathrm{s}$.[4] The antennas at both the sensors and the

---

[3]For simplicity, height differences between nodes and sensors are considered negligible with respect to the distance between them.

[4]Note how the number of degrees of freedom, $N_{\mathrm{dof}} = 2WT_{\mathrm{b}} = 400$, is considerably high in this configuration.

TABLE I
PROBABILITY OF CORRECT ESTIMATION OF THE NUMBER OF
TRANSMITTERS, $\widehat{T}$, AS A FUNCTION OF ρ AND σ.

$\rho \rightarrow$ $\sigma\text{(dB)} \downarrow$	1	1.2	1.4	1.6	1.8	2	2.2	2.4	2.6	2.8
1	0.83	0.98	0.98	0.99	1	1	1	1	1	1
3	0.78	0.97	0.98	0.99	0.99	1	1	1	1	1
5	0.69	0.91	0.94	0.95	0.99	1	1	1	1	1
7	0.57	0.73	0.87	0.91	0.94	0.97	0.98	0.99	1	1
9	0.37	0.48	0.72	0.75	0.83	0.83	0.86	0.88	0.94	0.95

target nodes are omnidirectional and the channel parameters are $\nu = 3$, $d_0 = 1\,\text{m}$, and $h_0 = -60.1\,\text{dB}$ [19]. The transmit power is the same for all nodes and equal to $P_{\text{tx}} = 10\,\text{dBm}$, while the noise power is $\sigma_{\text{n}}^2 = -93\,\text{dBm}$ for both nodes and sensors. The shadowing parameter σ is expressed in deciBel as $\sigma\text{(dB)} = 10\,\sigma/\ln 10$. Two types of packets are present in the target network, data packets with size $1024\,\text{Byte}$, and ACK packets of $112\,\text{Byte}$. Each node has an offered traffic of $1\,\text{Mb/s}$. Regarding the node counting process, the eigenvalue selection parameter is set to $w = 10^{-4}$ via scree plot [15], which ensures the best accuracy in the specific scenario, while in the RSS extraction phase, the threshold parameter is set to $q = 0.7$. The observation time is $T_{\text{ob}} = 1\,\text{s}$, which corresponds to $K = 100 \cdot 10^3$ power samples.[5] For grid-based search in the ML algorithm, the area is split into equal square cells of side $0.01\,\text{m}$. The parameters of the particle simulation algorithm where set to $h = 0.1$ and $N_{\text{iterations}} = 500$ according to [11].

All the results reported in this section are extracted by the simulations of $N_{\text{net}} = 2000$ different wireless networks where the position of the nodes and the sensors is random within the area with the only constraint that the nodes and sensors are spaced apart by at least $5\,\text{m}$. Fig. 3 shows an example of a simulation scenario with a network of $T = 5$ nodes and $S = 8$ sensors. The clouds of grey circles are position estimates of the nodes at different Monte Carlo (MC) instances using the proposed methodology with ML location estimation.

For each MC run, the localization error, defined as the Euclidean distance between the actual target position and the estimated one, and its root mean square error (RMSE) have been recorded.[6] Since both the sensors' and the nodes' spatial configuration significantly influence the position estimate, the localization error may deviate considerably from its average. Therefore, besides the average, 80-th and 20-th percentiles, standard deviation, and RMSE of the location error are also considered. The number of MC iterations for each network realization is 1000.

B. Number of Sensors and Shadowing

Our purpose is to study the effect of the number of sensors and the shadowing parameter on BSS and the localization performance. To make the results more understandable, we define the ratio $\rho = S/T$. In particular, in the simulations $T \in \{3, \ldots, 10\}$ and S is selected accordingly. The performance of the node counting is shown in Table I. In particular, the table reports the probability of correct counting, calculated as the
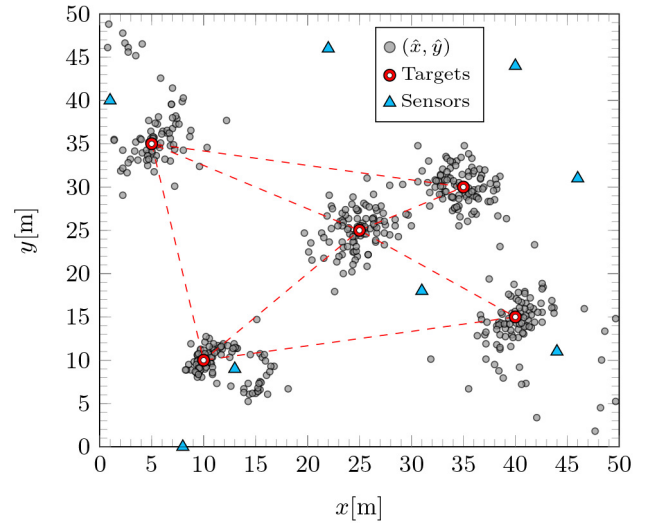
---

[5]We can estimate and update the target nodes position every $T_{\text{ob}} = 1\,\text{s}$.
[6]The RMSE for each MC simulation has been calculated over 200 independent realizations of shadowing.

Fig. 3. An example of scenario with $T = 5$, $S = 8$, and $\sigma = 3\,\text{dB}$. The red circles are the nodes of the network (or targets), the blue triangles are the RF sensors and the grey circles represent the estimate of the position of the nodes through the BSS-ML methodology.

ratio between the number of MC instances where the number of nodes is estimated correctly and the total number of MC instances, varying ρ and σ. As expected, the accuracy of the estimation degrades when the shadowing intensity σ increases, but such degradation can be counteracted by increasing the number of sensors.

The following results on localization performance are obtained considering 1000 MC instances with the correct node count. Fig. 4(a) shows the average value and the standard deviation of the localization error for the two proposed localization approaches and the solution based on particle simulation presented in [11], varying the ratio ρ. As it can be evinced, when ρ increases, the error decreases, showing that a larger number of sensors has a positive influence on the localization performance. Notably, the particle simulation algorithm requires a larger ρ to reach the same performance of the BSS-ML approach. Moreover, Fig 4(b) shows how increasing the shadowing parameter σ, the quality of the location estimation degrades significantly. Is it also shown how the ML approach can compensate the error due to the presence of strong shadowing with a further increase in ρ. Considering a mild shadowing regime with $\sigma = 1\,\text{dB}$, and $\rho = 4$, the average localization error drops down to $1\,\text{m}$ when the proposed methodology is combined with ML estimation. Instead, considering a strong shadowing scenario with $\sigma = 7\,\text{dB}$, the error reaches $9\,\text{m}$ with $\rho = 1.8$ and $5\,\text{m}$ with $\rho = 4$. In general, the BSS-ML approach performs better in all the scenarios, proving to be less sensitive to shadowing with respect to the BSS-LS and the particle simulation approach, and presenting an acceptable error for a RSS-based localization methodology.

It is also important to note that increasing ρ and decreasing σ the performance of the BSS improves with benefits on the localization step. As proof of this behavior, Fig. 4(c) compares the performance with the case of ideal separation (IS), i.e., considering a hypothetical BSS that perfectly reconstructs the transmitted power profiles. As can be noticed, increasing ρ, the
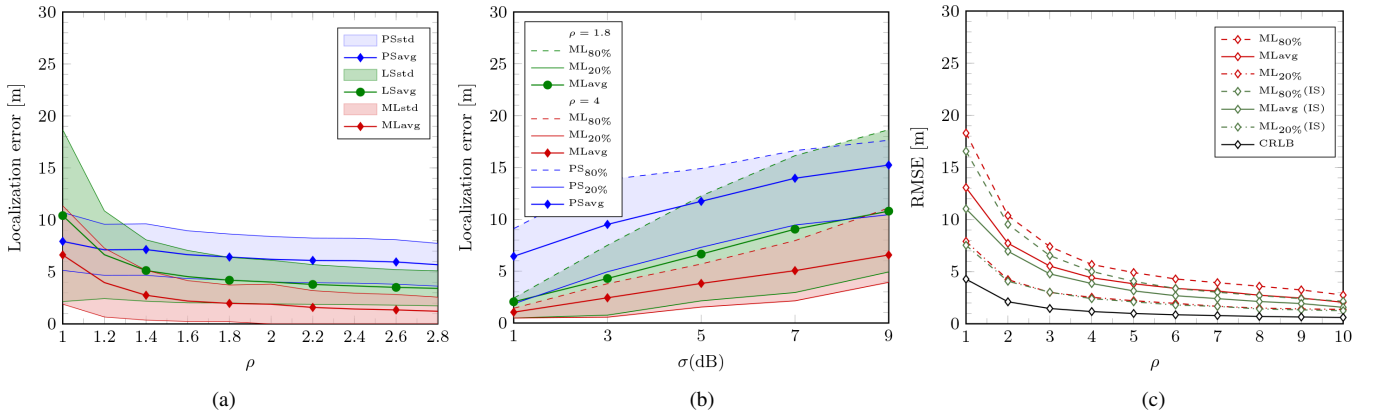
Fig. 4. (a) Comparison between the mean and the standard deviation of the localization error of the three algorithms (BSS-LS, BSS-ML and particle simulation (denoted as PS)) varying the ratio between the number of sensors and nodes, ρ, in a mild shadowing regime with $\sigma = 1$ dB. (b) The 20-th and 80-th percentiles and the mean localization error, for both BSS-ML and particle simulation, varying the shadowing parameter σ(dB) for $\rho = 1.8$ and $\rho = 4$. (c) The 20-th and 80-th percentiles and the RMSE of BSS-ML localization with the proposed BSS compared with the ideal BSS (denoted as IS) varying ρ with $\sigma = 5$ dB. The CRLB is used as a benchmark to assess the asymptotical improvement of the localization performance.

error introduced by the BSS decreases, and the performance obtained coincides with the ideal one. Moreover, in Fig. 4(c) the performance of the BSS-ML approach is compared to the CRLB [20, eq. (11)]. As expected, the proposed solution tends to approach the CRLB as ρ increases. For example, for $T = 1$ and $\rho = 50$ the RMSE deviates from the CRLB by 0.07 m.

Regarding the computational complexity, that of the particle simulation algorithm is $\mathcal{O}(STN_{\text{iterations}})$, while, e.g., that of our ML-based methodology is $\mathcal{O}(STN_{\text{grid}})$ where N_{grid} is the number of grid points. Thus, the complexities of the two algorithms are comparable despite presenting different localization performances.

V. CONCLUSION

This work proved that it is possible to localize nodes of a non-collaborative packet-based wireless network using only over-the-air power profiles captured by RF sensors. The novel framework combines RF sensing, BSS, RSS extraction, and RSS-based localization. The results confirmed the satisfactory performance of the proposed solution, showing how BSS combined with ML outperformed a state-of-the-art algorithm in realistic channels with noise and shadowing. Furthermore, we found that in a mild shadowing regime, even with relatively few sensors, i.e., $\rho \approx 1$, the localization error can be small when ML position estimation is adopted. Finally, we showed that the performance degradation due to BSS is tolerable considering that it offers the ability to locate multiple transmitters.

REFERENCES

[1] IEEE 802.22, "Standard for Wireless Regional Area Networks—Part 22: Cognitive Wireless RAN MAC and PHY specifications: P&P for operation in the TV Bands," Jul. 2011.

[2] E. Testi and A. Giorgetti, "Blind wireless network topology inference," *IEEE Trans. Commun.*, vol. 69, no. 2, pp. 1109–1120, Feb. 2021.

[3] E. Testi, E. Favarelli, and A. Giorgetti, "Blind source separation for wireless networks: A tool for topology sensing," in *Int. Conf. on Cog. Radio Oriented Wireless Net. (Crowncom)*, Online, Feb. 2021, pp. 1–14.

[4] E. Testi, L. Pucci, E. Favarelli, and A. Giorgetti, "Blind traffic classification in wireless networks," in *Proc. European Signal Processing Conference (EUSIPCO)*, Jan. 2021, pp. 1747–1751.

[5] A. Conti, S. Mazuelas, S. Bartoletti, W. C. Lindsey, and M. Z. Win, "Soft information for Localization-of-Things," *Proc. IEEE*, vol. 107, no. 11, pp. 2240–2264, Nov. 2019.

[6] M. Z. Win, F. Meyer, Z. Liu, W. Dai, S. Bartoletti, and A. Conti, "Efficient multisensor localization for the Internet of Things: Exploring a new class of scalable localization algorithms," *IEEE Signal Process. Mag.*, vol. 35, no. 5, pp. 153–167, Sep. 2018.

[7] S. Bartoletti, A. Conti, and M. Z. Win, "Device-free counting via wideband signals," *IEEE J. Sel. Areas Commun.*, vol. 35, no. 5, pp. 1163–1174, May 2017.

[8] S. Bartoletti, W. Dai, A. Conti, and M. Z. Win, "A mathematical model for wideband ranging," *IEEE J. Sel. Topics Signal Process.*, vol. 9, no. 2, pp. 216–228, Mar. 2015.

[9] C. An, Y. K. An, S.-M. Yoo, and B. E. Wells, "Efficient data association to targets for tracking in passive wireless sensor networks," *Ad Hoc Networks*, vol. 75-76, pp. 19 – 32, Jun. 2018.

[10] K. Magowe, A. Giorgetti, S. Kandeepan, and X. Yu, "Accurate analysis of weighted centroid localization," *IEEE Trans. Cogn. Commun. Netw.*, vol. 5, no. 1, pp. 153–164, Mar. 2019.

[11] P. Schulz, N. Franchi, and G. Fettweis, "RSS-based localization of multiple unknown transmitters through particle simulation," in *Proc. IEEE Int. Symp. on Joint Comm. & Sensing*, Dresden, Germany, Feb. 2021, pp. 1–6.

[12] H. Urkowitz, "Energy detection of unknown deterministic signals," *Proc. IEEE*, vol. 55, no. 4, pp. 523–531, Apr. 1967.

[13] A. Mariani, A. Giorgetti, and M. Chiani, "Effects of noise power estimation on energy detection for cognitive radio applications," *IEEE Trans. Commun.*, vol. 59, no. 12, pp. 3410–3420, Dec. 2011.

[14] G. L. Stuber, *Principles of Mobile Communication*, 2nd ed. Norwell, MA, USA: Kluwer Academic Publishers, 2001.

[15] I. T. Jolliffe, *Principal Component Analysis*. New York: Springer-Verlag, 2002.

[16] A. Hyvarinen, "Fast and robust fixed-point algorithms for independent component analysis," *IEEE Trans. Neural Netw.*, vol. 10, no. 3, pp. 626–634, May 1999.

[17] A. Giorgetti and K. Sithamparanathan, *Cognitive Radios Techniques: Spectrum Sensing, Interference Mitigation and Localization*. Artech House, Norwood, USA, 2012.

[18] M. Zafer, B. J. Ko, and I. W. Ho, "Transmit power estimation using spatially diverse measurements under wireless fading," *IEEE/ACM Trans. Netw.*, vol. 18, no. 4, pp. 1171–1180, Jan. 2010.

[19] M. Lacage and T. R. Henderson, "Yet another network simulator," in *Proc. Work. on Ns-2: the IP netw. sim. (WNS2)*, Pisa, Italy, Oct. 2006, p. 12–22.

[20] J. Wang, J. Chen, and D. Cabric, "Cramer-Rao bounds for joint RSS/DoA-based primary-user localization in cognitive radio networks," *IEEE Trans. Wireless Commun.*, vol. 12, no. 3, pp. 1363–1375, Feb. 2013.